Solar Phys (2014) 289:1349–1358
DOI 10.1007/s11207-013-0387-4

Coronal Holes in Solar Cycles 21 to 23

A. Tlatov · K. Tavastsherna · V. Vasil'eva

Received: 11 April 2013 / Accepted: 3 August 2013 / Published online: 30 August 2013

Abstract We present identifications of coronal holes (CHs) from observations in the He I 10 830 Å line made at Kitt Peak Observatory (from 1975 to 2003) and in the EUV 195 Å wavelength with SOHO/EIT (from 1996 to 2012). To determine whether a feature is a CH we have developed semi-automatic techniques for delineating CH borders on synoptic charts and for subsequent mapping of these borders on magnetic-field charts. Using these techniques, we superimposed CH borders on magnetic-field charts over the time interval from 1975 to 2012. A major contribution to the total area was made by high-latitude CHs, but in the declining phase of solar cycle 23, the contribution from low-latitude CHs increased substantially. Variations in the flux of Galactic cosmic rays and those in the inclination angle of the heliospheric current sheet followed the cyclic variations of CH areas. High-latitude CHs affect the properties of the solar wind in the ecliptic plane.

Keywords Coronal holes · Solar cycle · Solar wind

1. Introduction

Observations made with coronagraphs and during solar eclipses (Waldmeier, 1975), EUV and X-ray observations made with space missions, spectroheliograms in the He I 10 830 Å line, and radio observations indicate that coronal holes (CHs) represent an important index of solar activity. CHs are long-lived extended structures with decreased temperature and abnormally low density (Cranmer, 2009), localized in the regions of large-scale unipolar magnetic fields with open field lines that do not inhibit the radial expansion of coronal plasma (Harvey and Sheeley, 1979; Insley, Moore, and Harrison, 1995;

A. Tlatov (✉) · V. Vasil'eva
Kislovodsk Mountain Astronomical Station of Pulkovo Observatory, Gagarina str. 100, Kislovodsk, Russian Federation
e-mail: tlatov@mail.ru

K. Tavastsherna
Pulkovo Astronomical Observatory, Russian Academy of Sciences, Pulkovskoe sh. 65, St. Petersburg 196140, Russian Federation
e-mail: tavastsherna@rambler.ru

Obridko and Shelting, 1989). CHs are sources of high-speed solar wind (with the average velocity around 700 km s^{-1} and a decreased plasma density $n \approx 4$ cm^{-3}), which noticeably affects the Earth's magnetosphere (Wilcox, 1968; Nolte *et al.*, 1976; Sheeley, Harvey, and Feldman, 1976; Sheeley and Harvey, 1981; Wang and Sheeley, 1990). CHs are responsible for the formation of recurrent particle flows that regularly appear with a period of approximately 27 days and exist for several months. EUV radiation in a CH region displays decreased intensity, which may be related to both the reduced temperature (0.8×10^6 K) and the density depleted to 0.25 of that in a quiet corona (Cranmer, 2009). Hence it follows that it is a challenging problem to identify and delineate CHs from observations of the Sun and determine their parameters, such as their location, area, latitudinal and longitudinal size, magnetic field, *etc*.

2. Data and Analysis Methods

CHs are detected on the data from ground-based telescopes in the He I 10 830 Å line and with satellite-borne EUV observations. Here, we present our identifications of CHs from the 1975 – 2003 observations at Kitt Peak (Kitt Peak Vacuum Telescope, KPVT) and from SOHO/EIT Fe XII 195 Å observations (1996 – 2012). We also used the He I 10 830 Å data obtained with the SOLIS telescope (the successor of KPVT, also at Kitt Peak) from 2004 to 2012, when no SOHO/EIT observations were made. The synoptic maps of the KPVT and SOHO/EIT observations are available in FITS format at ftp://nsokp.nso.edu/kpvt/synoptic; http://www2.ess.ucla.edu/, the synoptic maps of SOLIS data can be retrieved at http://solis.nso.edu/jingli/LSM/vsm-maps.php.

Identifying CHs is difficult. CHs are characterized by a lower electron density and temperature than typical quiet-Sun regions; for this reason, they look bright in the He I 10 830 Å line and dark at EUV and X-ray wavelengths (Zirker, 1977). Nonetheless, this criterion does not make it possible to distinguish CHs unambiguously from other similar regions on the Sun. For example, a light area in the He I 10 830 Å spectroheliograms might indicate not only a CH, but also a filament channel, which at EUV wavelengths also looks dark. In addition, CHs may not display sharp boundary patterns and may be partly obscured by active region loops. At different wavelengths, CHs look slightly different in their shape and area (Kahler, Davis, and Harvey, 1983).

Initially, CHs were identified visually by experienced observers (Harvey and Recely, 2002; McIntosh, 2003); recently, however, several automatic methods have been suggested. Some of them are based on the fixed intensity threshold at a given wavelength (Abramenko, Yurchyshyn, and Watanabe, 2009). This technique, however, has proven insufficient (de Toma, 2011). In other methods, more complicated approaches are used (de Toma and Arge, 2005; Henney and Harvey, 2005). For example, from observations in the He I 10 830 Å line (Henney and Harvey, 2005), pixels with intensity above 1/10 of the median intensity over the image are initially selected, and subsequent smoothing and filtering procedures are applied. A technique developed for CH identification from EUV data (de Toma, 2011) also uses a variable threshold level that varies from one chart to another; the threshold is determined as the width of the Gaussian distribution of the pixel intensity, with a factor depending on the wavelength.

We tested different methods of CH identification and finally concluded that a totally automatic determination of the threshold level is insufficient. We developed a semi-automatic technique for delineating CH borders on synoptic charts and for superimposing these borders on magnetic-field charts.

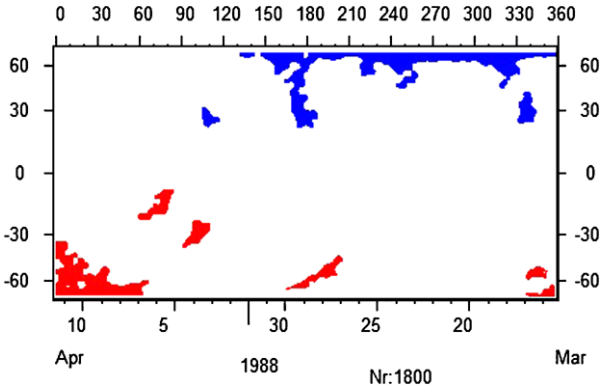

Figure 1 A synoptic chart for Carrington rotation No. 1800. Coronal holes of positive and negative polarities of the magnetic field are indicated with red and blue colors, respectively.

Our method consists of several steps. Initially, we used a smoothing procedure for adjacent pixels with a smoothing width of approximately 3 heliographic degrees. At the first step, we selected a suggested threshold intensity level $I_{\rm th}$, which was determined from the pixel intensity histogram $H(I)$. Then we took the logarithm of the cumulative histogram $P = \log(\sum H(I))$ and selected the threshold level $I_{\rm th}$ that corresponded to the largest difference $P_{i+1} - P_i$ of the logarithmic cumulative histogram. In a second step, a supervisor manually corrected the selection of the threshold intensity $I_{\rm th}$. As a rule, the correction was carried out on the maps with a large number of gaps in observation days. Then, also in the manual mode, we filtered out filaments seen as low-intensity zones at EUV wavelengths, and filament cavities seen as bright structures in the He I 10 830 Å line. To this end, we superimposed the position of the neutral line of the large-scale magnetic field derived from the Hα synoptic maps obtained at Kislovodsk Mountain Astronomical Station.[1] At the final stage, we filtered out regions with an area smaller than 10^{-3} in units of the solar hemisphere area. The selected regions were combined into a single structure with a common border. These structure parameters were recorded in vector format, which allowed us to transfer them to the maps of other observations. If necessary, the observer can edit the boundaries of individual regions. For the times when there were no observations, the operator may copy onto the map the CH boundaries from the previous rotation or from CH maps obtained by the other telescopes.

The data were digitized independently by two observers to increase the accuracy in ambiguous situations; in general, both results appeared to be identical. In total, we identified 3 943 CHs from KPVT (1975 to 2003 observations) and 1 884 CHs on SOHO/EIT 195 Å synoptic charts. In the absence of SOHO/EIT observations, the data were supplemented by CHs derived from SOLIS observations. Figure 1 presents an example of a CH synoptic chart for the Carrington rotation No.1800.

3. Results

The number, sizes, and latitudinal positions of CHs vary depending on the phase of the solar cycle. CHs with the largest area occur at high latitudes within five to six years around the minimum of the solar cycle; they disappear closer to the cycle maximum. At the declining

[1] http://www.solarstation.ru.

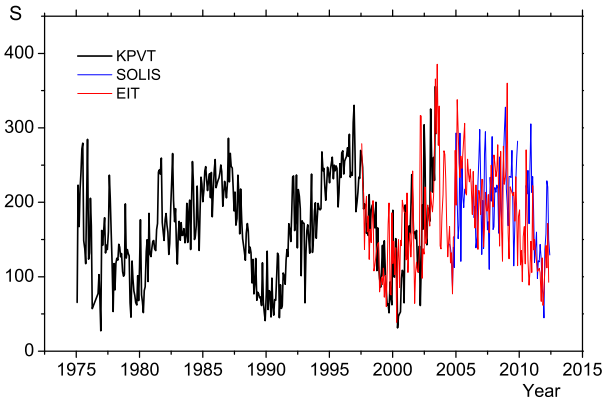

Figure 2 CH areas derived from the Kitt Peak Vacuum Telescope (KPVT) data (1975 to 2003), SOHO/EIT data (1996 to 2012), and SOLIS data (2004 to 2012) in units of 10^{-3} of the solar hemisphere, averaged over one Carrington rotation.

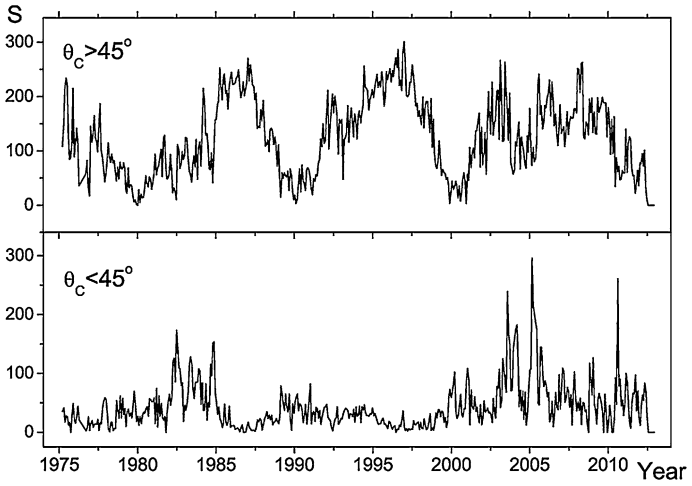

Figure 3 CH areas averaged over one solar rotation in units of 10^{-3} of the solar hemisphere for a combined data set of KPVT He I 10 830 Å and SOHO/EIT 195 Å. Top: the area of circumpolar CHs (geometrical center θ_c above 45°). Bottom: the area of low-latitude CHs ($\theta_c < 45°$).

phase of solar activity, a gradual growth of CHs with new polarity is observed. Figure 2 presents the CH areas derived from KPVT He I 10 830 Å observations (1975 to 2003) and from SOHO/EIT 195 Å observations (1996 to 2012). The two data series overlap in the interval 1997 to 2003, in which they display sufficient consistency (Figure 2). Also presented are the CH areas from SOLIS from 2004 to 2012[2] (Henney and Harvey, 2005). The CH areas (S) observed in these two wavelengths are related as $S_{\mathrm{He\,10\,830}} \approx 0.9 S_{\mathrm{EIT195}}$.

We have created a series of synoptic maps during the years 1975 – 2012 (Carrington rotations 1625 – 2123). This series combines the observations in the He I 10 830 Å line and SOHO/EIT observations when overlapping data were available from KPVT. For periods that lack data and after 2003 we used only SOHO/EIT 195 Å data. Figure 3 presents the CH areas at low ($\theta_c < 45°$) and high ($\theta_c > 45°$) latitudes, where θ_c denotes the latitude (absolute value) of the geometrical center of a CH. The low-latitude CHs in solar cycles 21 and 23 display

[2] http://solis.nso.edu/vsm.

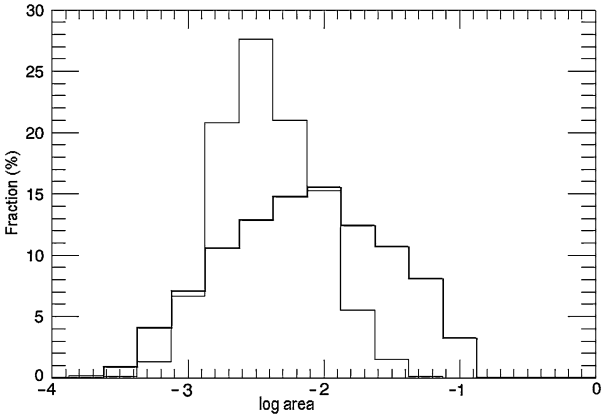

Figure 4 The histogram of CH areas in units of the solar hemisphere. Thick and thin lines indicate high-latitude ($\theta_c > 50°$) and low-latitude ($\theta_c < 40°$) CHs.

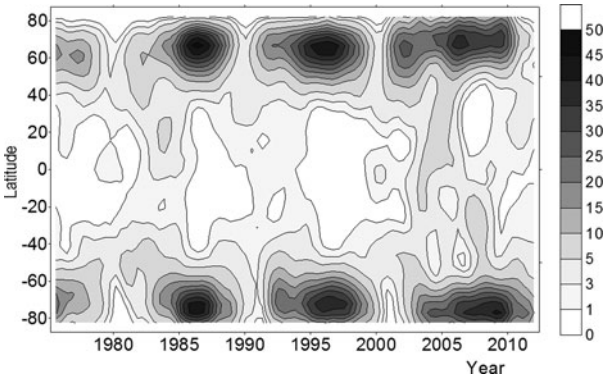

Figure 5 The time–latitude distribution of CH areas in units of 10^{-3} of the solar hemisphere, calculated from synoptic charts in 5° latitude intervals.

the largest area at the declining activity phase, with the largest area within the intervals 2003 to 2004 and 2005 to 2006.5. The increase in the area of the low-latitude CHs in these years was also reported by Abramenko *et al.* (2010).

The characteristic areas for high- and low-latitude CHs are different (Figure 4). While the area distribution of the low-latitude CHs peaks at $S \approx 3 \times 10^{-3}$ of the solar hemisphere, for high-latitude CHs the peak is at $S \approx 10^{-2}$.

CHs, as a rule, are located in the regions of a large-scale unipolar magnetic field. Therefore, during solar minima they are seen in circumpolar regions, at latitudes higher than 60° (Figure 5). At the time of the polar magnetic-field reversal, high-latitude CHs disappear and then occur again two to three years later. At middle and low latitudes, CHs appear at the declining phase of the cycle. However, in contrast to the high-latitude CHs, they have no clearly defined latitude zone where they occur more often.

The parameters of the magnetic field that underlies CHs are important. To determine them, we superimposed the CH borders on synoptic charts of magnetic fields obtained from KPVT (1975 to 2003), SOLIS (2004 to 2012), and SOHO/MDI when there were no other data. The synoptic charts of the magnetic fields for the year 2003 from SOHO/MDI were reduced to the 360 × 180-pixel format of KPVT magnetograms. Observations with different magnetographs may have systematic differences, especially at high latitudes. Nevertheless, in this article, the data were not reduced to a uniform system. Figure 6 shows the average

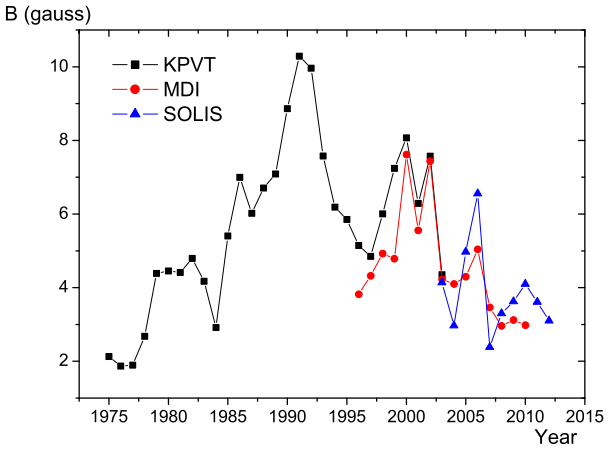

Figure 6 The annual mean values of the area-averaged magnetic-flux density in CHs derived from KPVT, SOHO/MDI, and SOLIS data.

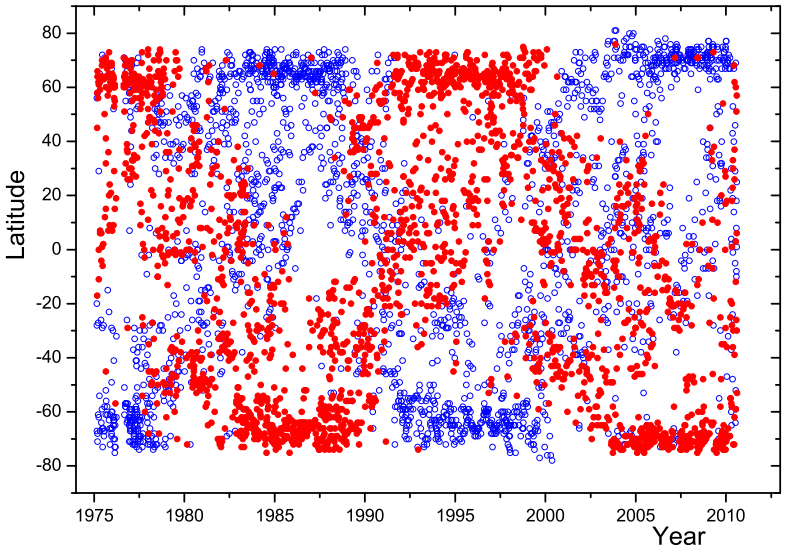

Figure 7 Time–latitude distributions of CH centers. CHs of positive (negative) polarity are marked with red (blue).

annual magnetic-flux density in CHs determined from observations of the three magnetographs. The highest flux density there is found in the period of maximum solar activity.

At the maximum and the declining phases of a cycle, the geometrical centers of CHs of the same magnetic polarity move from one pole to the other. For example, in 1988 – 1993, CHs with negative polarity drifted from the north to the south pole, while those with positive polarity moved in the opposite direction (Figure 7). This effect might be interpreted as the rotation of the large-scale dipole field during a solar cycle (Livshits and Obridko, 2006). However, the longitudinal distributions of CH centers display no systematic motions that would distinguish their magnetic polarity (Figure 8).

The average magnetic flux in CHs varies from one cycle to another. Figure 9 presents the variations of the magnetic flux in CHs in units of 10^{20} Mx (maxwell). In spite of relatively

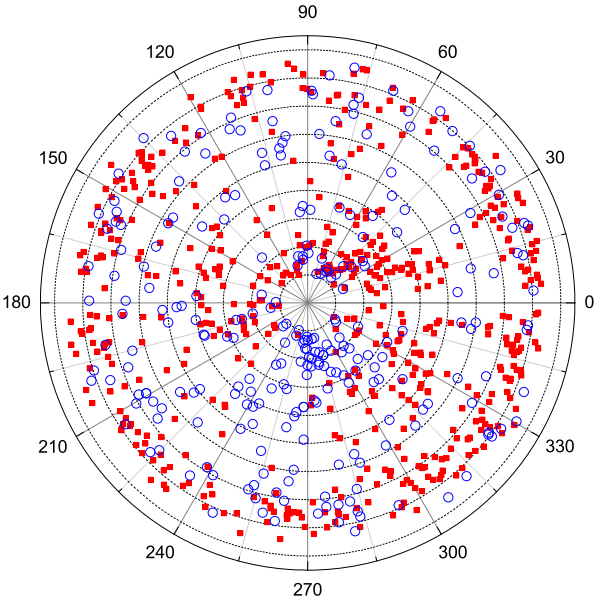

Figure 8 Positions of CH centers in 1988 – 1993 seen from the north pole of the Sun. CHs of positive (negative) polarity are marked with red (blue).

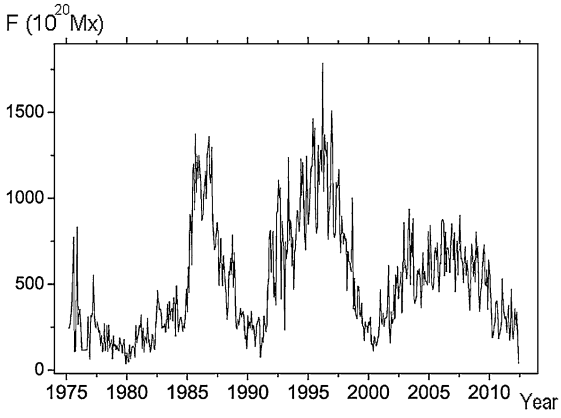

Figure 9 Magnetic flux of coronal holes calculated for each synoptic map.

large areas of CHs in cycle 23, the magnetic flux in CHs in this cycle was substantially lower than that in the previous cycles.

4. Discussion and Conclusions

Coronal holes (CHs) are solar regions with an open magnetic field. Studying their characteristics and evolution is important for understanding the nature of the solar magnetic field and the mechanisms of acceleration and heating of the solar wind. The evolution of CHs also has implications for the Earth's magnetosphere. On the basis of synoptic observations made at Kitt Peak Observatory and of EUV observations of SOHO/EIT 195 Å, we have composed a catalog of CHs in the time interval from 1975 to 2012, which includes three complete cycles (21, 22, and 23) of solar activity. The He I 10 830 Å line data of Carrington rotations

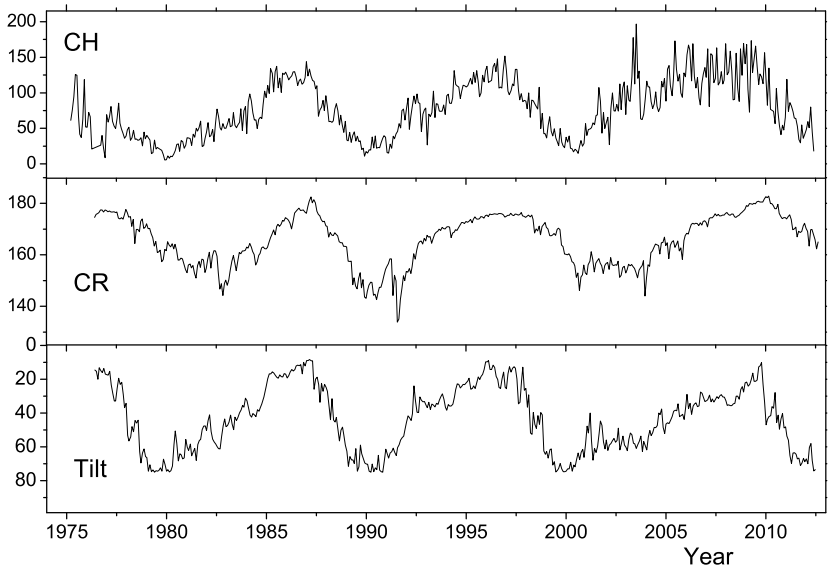

Figure 10 Comparison between the CH area at latitudes $\theta > 60^\circ$ (top), the Galactic cosmic-ray flux (middle), and the inclination angle of the heliospheric current sheet calculated from the Wilcox Solar Observatory data (bottom).

No. 1625 to 2003 and EIT 195 Å observations for rotations 1909 to 2123 were collected at the site of Kislovodsk Mountain Astronomical Station.

The obtained data series makes it possible to compare the CH evolution with the parameters of solar activity and the solar wind. Figure 10 presents a comparison of our synthesized CH area, the galactic cosmic ray flux derived from the data of the Kiel neutron monitor, and the inclination angle of the heliospheric current sheet calculated at the height $R = 2.5 R_\odot$ from the data of Wilcox Solar Observatory.[3] in cycles 21 and 22, the latter two indices of solar activity agree well with the CH area. In cycle 23, the agreement deteriorates somewhat, which may be caused by a variation in the average magnetic flux in CHs (Figure 9).

CHs are known to be a source of the high-speed solar wind (Nolte *et al.*, 1976; Sheeley, Harvey, and Feldman, 1976). Generally, this is explained by the contributions from circumequatorial CHs, which may accelerate the plasma in the ecliptic plane. Indeed, in the time interval 2003 – 2004, low-latitude CHs were responsible for the increase in the solar wind velocity (Abramenko, Yurchyshyn, and Watanabe, 2009; Manoharan, 2010). However, our analysis shows that a polar CH may also influence the solar wind in the vicinity of the ecliptic plane. Figure 11 presents the areas of circumpolar CHs at latitudes exceeding 60° compared with the variations of the magnetic Mach number of the solar wind, according to the OMNI2 data.[4] The comparison indicates the good correlation of these parameters. It is possible that the magnetic field of polar CHs causes the compression of the solar wind flux toward the solar equator and thus influences the properties of the solar wind at all latitudes (Tlatov, 2010). Additional research is needed to clarify the physical connections between CHs and the solar wind parameters.

[3] http://wso.stanford.edu/tielts.html.

[4] http://nssdc.gfc.nasa.gov/omniweb.

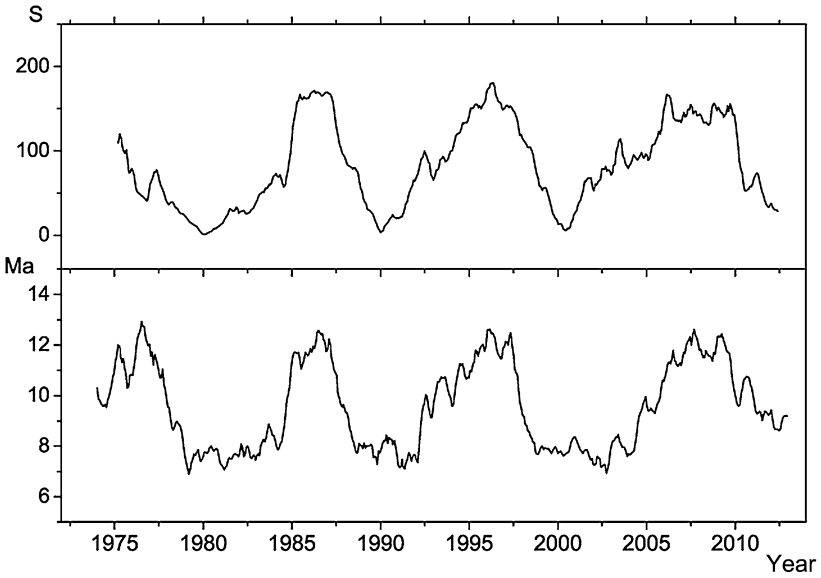

Figure 11 Comparison between the areas of polar CHs at latitudes $\theta > 60°$ (top) and the variations of the magnetic Mach number of the solar wind (bottom). The data were smoothed with the sliding window of six solar rotations.

In solar cycle 23, the total CH area is large (Figure 2), with a substantial fraction of the areas of low-latitude CHs (Figure 3). However, in spite of this large CH area, the total magnetic flux at the minimum between cycles 22 and 23 was substantially lower than the flux in the previous cycles. This is probably due to a decrease in the intensity of the polar magnetic field (Figure 6). In the years 2003 to 2004, an increase in the solar wind velocity was observed along with the relatively large area of low-latitude CHs (Figure 3). At the same time, however, the magnetic flux in CHs remained at a low level (Figure 9), which may be the reason why the increase in the wind velocity did not result in any noticeable growth of the geomagnetic activity (Manoharan, 2010).

Acknowledgements The work was supported by the Russian Foundation for Basic Research (RFBR), the Russian Academy of Sciences, and the Program to Support Leading Scientific Schools by the Russian Federal Agency for Science and Innovations. We are also indebted to Dr. K. Maslennikov for his assistance in preparing the English version of the manuscript.

References

Abramenko, V., Yurchyshyn, V., Watanabe, H.: 2009, *Solar Phys.* **260**, 43.
Abramenko, V., Yurchyshyn, V., Linker, J., Mikiè, Z., Luhmann, J., Lee, C.O.: 2010, *Astrophys. J.* **712**, 813.
de Toma, G.: 2011, *Solar Phys.* **274**, 195.
de Toma, G., Arge, C.N.: 2005, In: Sankarasubramanian, K., Penn, M., Pevtsov, A. (eds.) *Large-Scale Structures and Their Role in Solar Activity*, *ASP Conf. Ser.* **346**, 251.
Cranmer, S.: 2009, *Living Rev. Solar Phys.* **6**(3). http://solarphysics.livingreviews.org/Articles/lrsp-2009-3/.
Kahler, S.W., Davis, J.M., Harvey, J.W.: 1983, *Solar Phys.* **87**, 47.
Harvey, K.L., Recely, F.: 2002, *Solar Phys.* **211**, 31.
Harvey, J.W., Sheeley, N.R., Jr.: 1979, *Space Sci. Rev.* **23**, 139.
Henney, C.J., Harvey, J.W.: 2005, In: Sankarasubramanian, K., Penn, M., Pevtsov, A. (eds.) *Large-Scale Structures and Their Role in Solar Activity*, *ASP Conf. Ser.* **346**, 261.

Insley, J.E., Moore, V., Harrison, R.A.: 1995, *Solar Phys.* **160**, 1.
Livshits, I.M., Obridko, V.N.: 2006, *Astron. Rep.* **50**, 926.
Manoharan, P.K.: 2010, *Astrophys. J.* **751**, 13.
McIntosh, P.S.: 2003, In: Wilson, A. (ed.) *Solar Variability as an Input to the Earth's Environment, International Solar Cycle Studies Symposium* **SP-535**, ESA, Noordwijk, 807.
Nolte, J.T., Krieger, A.S., Timothey, A.F., Gold, R.E., Roelov, E.C.: 1976, *Solar Phys.* **46**, 303.
Obridko, V.N., Shelting, B.D.: 1989, *Solar Phys.* **124**, 73.
Sheeley, N.R., Jr., Harvey, J.W., Feldman, W.C.: 1976, *Solar Phys.* **49**, 271.
Sheeley, N.R., Jr., Harvey, J.W.: 1981, *Solar Phys.* **70**, 237.
Tlatov, A.G.: 2010, *Astrophys. J.* **714**, 805.
Waldmeier, M.: 1975, *Solar Phys.* **40**, 351.
Wang, Y.-M., Sheeley, N.R., Jr.: 1990, *Astrophys. J.* **355**, 726.
Wilcox, J.M.: 1968, *Space Sci. Rev.* **8**, 258.
Zirker, J.B. (ed.): 1977, *Coronal Holes and High-Speed Wind Streams* **5**, Colorado Assoc. Univ. Press, Boulder.